Vol. 314: 77–88, 2006 | MARINE ECOLOGY PROGRESS SERIES
Mar Ecol Prog Ser | Published May 22

Down-mixing of phytoplankton above filter-feeding mussels—interplay between water flow and biomixing

Johan Lassen[1], Martin Kortegård[1], Hans Ulrik Riisgård[1,*], Michael Friedrichs[2], Gerhard Graf[2], Poul S. Larsen[3]

[1]Marine Biological Research Centre (University of Southern Denmark), Hindsholmvej 11, 5300 Kerteminde, Denmark
[2]Institute of Biological Sciences, Marine Biology, University of Rostock, Albert-Einstein-Strasse 3, 18059 Rostock, Germany
[3]Department of Mechanical Engineering, Fluid Mechanical Section, Technical University of Denmark, Building 403, 2800 Kgs. Lyngby, Denmark

ABSTRACT: Filter-feeding bivalves may have a pronounced grazing impact on the phytoplankton biomass in many shallow marine areas. The blue mussel *Mytilus edulis*, which lives in dense beds, can filter more than 100 m^3 m^{-2} d^{-1}, but the grazing impact is highly influenced by hydrodynamic processes. Without externally generated currents or turbulent mixing, only a thin layer of near-bottom water would be subject to the down-mixing that causes an important supply of food to the mussels. Here, food-depleted jets of water expelled through the exhalant opening of a mussel may not only prevent the water, once filtered, from re-entering the animal, but the substantial speed of the jet may also help to mix the near-bottom water. The extent of such biological mixing—'biomixing'—caused by a dense population of *M. edulis* (200 cm long bed, filtering at 147 m^3 m^{-2} d^{-1}) was studied experimentally at 2 flow speeds (4 and 8 cm s^{-1}) in a laboratory flume channel at natural (low) algal concentrations in order to determine its relative importance compared to current-generated turbulence. Distributions of algal cells a distance of 162 cm from the start of the bed showed a near-bottom depletion of about 58 and 45%, respectively, for the 2 flow speeds, which indicate the degree of refiltration. In addition, flow structures were quantified in terms of distributions of velocity, turbulent shear stress and turbulent kinetic energy in the benthic boundary layer at 3 levels of mussel filtration-activity (maximal, reduced and zero). A description is given of this filtration activity of *M. edulis* with and without added suspensions of algal cells, which influence its valve-opening degree and filtration rate. It is concluded that biomixing enhances the flow-induced down-mixing of phytoplankton and can be identified as peaks in profiles of turbulent kinetic energy and turbulent shear stress. The associated increase in friction velocity over the length of the mussel bed at maximal filtration activity amounted to 56 and 49% for the 2 flow speeds studied. This shows the functionality of biomixing to be most helpful at low speed, where it is most needed due to the low levels of flow induced turbulence contributing to down-mixing of phytoplankton.

KEY WORDS: *Mytilus edulis* · Boundary layer · Flume · Turbulent mixing · Grazing impact · Filtration activity · Refiltration · Exhalant jets

INTRODUCTION

Benthic filter-feeding macro-invertebrates, such as bivalves, ascidians and some polychaetes, often play a significant ecological role in coastal waters because they extract large quantities of phytoplankton from the water. Dense populations of filter-feeding zoobenthos can exert a considerable grazing impact, and typically the area-specific population filtration rate is between 1 and 10 m^3 water m^{-2} d^{-1} or more, equivalent to a vol-

*Corresponding author. Email: hur@biology.sdu.dk

ume that may be several times the overlying water column (e.g. Jørgensen 1984, 1990, Petersen & Riisgård 1992, Riisgård 1991, 1998, Norén et al. 1999, Dolmer 2000, Forster 2004). A recent study by Riisgård et al. (2004) evaluated the grazing impact of filter-feeding animals in the shallow Odense Fjord (Denmark). This fjord is characterised by large biomass of filter-feeding polychaetes *Nereis diversicolor*, clams *Mya arenaria* and cockles *Cerastoderma glaucum*. Based on recorded population densities, and assuming efficient vertical mixing, it was found that the half-life for phytoplankton was less than 3 h in the inner part of the fjord. But it is obvious that this potential grazing impact also depends on hydrodynamic processes, such as currents and mixing of the overlying water. The grazing impact is enhanced by turbulent mixing of the water mass due to wind-, wave- and current action, coupling the benthic filter feeders to the pelagic biomasses. A key to the understanding of spatial and temporal variations in pelagic biomasses is the knowledge of the circumstances under which such a coupling or decoupling of benthic filter feeders takes place (Peterson & Black 1988, Loo & Rosenberg 1989, Butman et al. 1994, Møhlenberg 1995, Riisgård et al. 1996a,b, 1998).

To date, a number of attempts have been made to model phytoplankton-concentration gradients caused by filter-feeding bivalves in relatively strong currents with a high degree of turbulence (Wildish & Kristmanson 1984, Fréchette & Bourget 1985, Fréchette et al. 1989, O'Riordan et al. 1993, Butman et al. 1994, Mann & Lazier 1996, Wildish & Kristmanson 1997, Herman et al. 1999, Tweddle et al. 2005). Moderate currents may generate enough turbulence in the benthic boundary layer to increase the supply of food to the filter feeders by turbulent mixing. However, the additional 'biomixing' induced by the filter feeders themselves, if they are living in areas dominated by relatively low current regimes, has not yet been included in any model. It has often been supposed that the food-depleted jets of water expelled through exhalant openings of benthic filter feeders prevent the filtered water from reentering the animal (Vogel 1994). But another or complementary function of these jets (which can reach a substantial speed) may be to mix the near-bottom water. The extent of this biomixing has not yet been thoroughly examined, although the degree to which exhalant jets affect the vertical mixing and thus the transport of phytoplankton down to the bottom can play a crucial role in determining the actual grazing impact of benthic filter feeders (Larsen & Riisgård 1997).

A diffusion model was used by Larsen & Riisgård (1997) to describe the development of vertical profiles of phytoplankton above filter-feeding benthic animals in stagnant water. This diffusion model helps to improve our understanding of benthic filter feeding under conditions where biomixing dominates over current-generated turbulence. However, in the presence of flow and when the concentration gradient is primarily caused by the current-generated turbulence, the distribution of phytoplankton requires a modelling of the convection-diffusion process, including the filter-feeding-induced biomixing, which may in turn enhance the flow-induced mixing. The magnitude of inferred values of effective diffusivity from the modelling results of Larsen & Riisgård (1997) suggests that biomixing could also enhance the flux in situations with flow-induced mixing.

Phytoplankton distributions have been recorded in flume experiments above pairs of in- and exhalant silicone tubes representing populations of filter-feeding clams (Monismith et al. 1990, O'Riordan et al. 1993, 1995), and above live mussels (Butman et al. 1994). The purpose of using 'model animals' was to study the formation of a concentration boundary layer at a constant and known benthic filtration rate (O'Riordan et al. 1993, 1995) thereby circumventing the problems that Butman et al. (1994) encountered with a reduced filtration activity of mussels during experiments due to insufficient algal supply. But, having kept the mussel bed in the flume for several mo prior to the experiment, van Duren et al. (2006) did not encounter such problems in their flume study of the boundary layer structure over a bed of filter-feeding mussels and they found that filtration activity may have an important effect on exchange processes in the near-bottom region. There is now evidence that filter-feeding bivalves maintain a constantly high filtration rate in the presence of natural (low) concentrations of phytoplankton (Riisgård & Randløv 1981, Clausen & Riisgård 1996, Riisgård 2001a,b, Riisgård & Seerup 2003, Riisgård et al. 2003). For *Mytilus edulis*, a phytoplankton range between the lower starvation level of about 0.5 µg Chl *a* l^{-1} and the upper saturation level of about 5 µg Chl *a* l^{-1} secures a maximal filtration rate (Clausen & Riisgård 1996, Riisgård et al. 2003) whereas both starvation and saturation lead to reduced valve gape and thus to a reduction in the filtration rate.

The aim of the present project was to study experimentally the relative importance of biomixing caused by fed, starved and dead mussels (i.e. with maximal, reduced and zero filtration activity) in relation to low and high levels of current-generated turbulence under controlled conditions in a laboratory flume. Such results are suggested to be important for a better understanding of the interaction between grazing impacts of benthic filter feeders and near-bottom flow conditions. The importance of biomixing has been ascertained by comparing turbulent flow properties for different mussel filtration activities under typical near-bottom flow conditions.

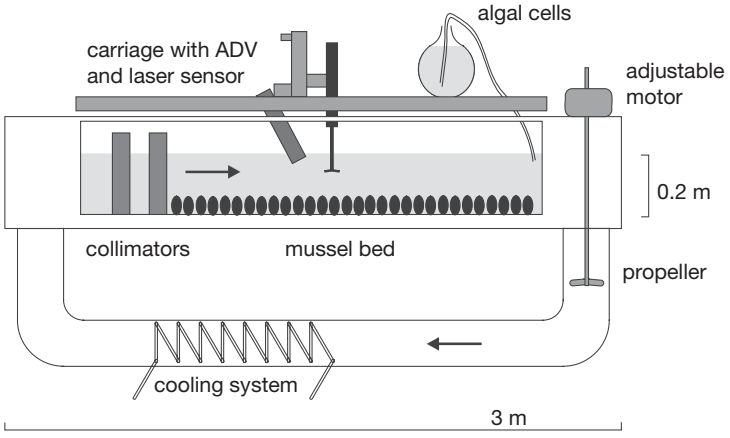

Fig. 1. Sketch of flume channel with mussels in the test section (2 m long, 0.4 m wide, 0.2 m water depth, 360 l total volume)

MATERIALS AND METHODS

Flume experiments. The present study used a recirculating flume channel at the University of Rostock (total water volume 360 l; Springer et al. 1999) equipped with a 2 m long, 0.4 m wide and 0.2 m deep test section, with mussels placed on thin removable plates (Fig. 1). Flow is generated by a propeller capable of producing flow speeds in the range of 1 to 20 cm s^{-1}. Two collimators upstream of the test section and honeycomb grids at both ends of the return pipe serve to reduce the free-stream turbulence in the test section. A 3-dimensional computer-controlled carriage supports and positions the sensors that consist of (1) a downward-looking 3-beam NorTek ADV (Acoustic Doppler Velocimeter) working at 10 MHz, which has a sampling volume situated 5 cm below the sensor head, and (2) a bottom scanning laser relief sensor with a resolution in the sub-millimetre range (Friedrichs & Graf 2006). The ADV simultaneously measures the axial, transverse and vertical velocity components. A cooling unit and layers of insulating foam control the water temperature, which in the present study was kept at 10°C. The salinity was adjusted to 20 psu. For the coordinate system employed, the axial distance x = 0 denotes the leading edge of the mussel bed and the vertical distance z = 0 the flume floor.

Mussels. Approximately 1000 blue mussels *Mytilus edulis* collected at Pughavn/Fyns Hoved (Denmark) with an average shell length of 4.8 ± 0.5 cm were transferred to the flume in Rostock. Table 1 shows the density, average shell length and calculated area-specific population filtration rate (F_{pop}) of the mussels in the flume test section. The average height of the mussel bed was 3.9 ± 1.1 cm. F_{pop} was calculated as $\sum F_{ind}$/area, where the individual filtration rate of a mussel (F_{ind}, l h^{-1}) of shell length L_s (mm) was calculated according to Kiørboe et al. (1981, corrected in Riisgård 2001a) as: $F_{ind} = 0.0012 L_s^{2.14}$. The mussels were allowed to acclimate for 5 d before the experiments were started. In this period, they were fed with a monoculture of *Rhodomonas* sp. for a few hours d^{-1} at concentrations between 2000 and 5000 cells ml^{-1}.

Experimental design. The effect of mussel biomixing on the momentum and concentration boundary layer characteristics above the mussel bed was revealed by comparing results of flow and algal concentration above the mussel bed for a 3 × 2 experimental matrix, comprising 3 states of mussel filtration activity (maximal, reduced, zero) and 2 flow rates in terms of depth-averaged velocity (slow: 4 cm s^{-1}, fast: 8 cm s^{-1}).

Flow measurements. For the 3 × 2 experimental matrix, the ADV was repeatedly used to record profiles of the local velocity components (axial, transverse and vertical) at high resolution at 4 downstream positions above the mussel bed: x = 28, 75, 121, and 168 cm. The height steps in these vertical profiles were increased from 0.5 cm in a lower part (1.63 to 8.63 cm above the flume floor) to 1 cm in the upper part (8.63 to 13.63 cm). At each location, sampling periods of 30 s at 20 Hz produced 600 data samples for each velocity component from which statistical mean values and covariance (Reynolds stress) were computed. Sediment particles (silt) were added in order to avoid particle depletion in the flume due to the mussel filtration, and hence to keep the level of acoustic backscattering high enough for a correct operation of the ADV.

Algal concentration measurements. For the experimental scenarios with maximal and zero filtration activity of mussels, the local mean algal concentration was measured to give vertical profiles at 5 downstream positions: x = 0, 28, 76, 122, and 162 cm. The height steps in these vertical profiles were 2 cm from 2 to 20 cm above the flume floor. These profiles were obtained by simultaneous gravimetric sampling of the water from all heights through thin silicone tubes protruding from the wall of a rigid plastic pipe inserted

Table 1. *Mytilus edulis*. Mussel density (D), average shell length (L_s) ± SD, and estimated area-specific population-filtration rate (F_{pop}) along the flume mussel bed, starting at x = 0

x (cm)	D (ind. m^{-2})	L_s ± SD (mm)	F_{pop} (m^3 m^{-2} d^{-1})
0–50	1262	47 ± 5.3	147
51–100	1564	48 ± 5.0	182
101–150	1195	48 ± 4.9	139
151–200	1021	48 ± 4.7	119

vertically into the flow. The sampling time per vertical profile was approximately 3 min. The water samples, consisting of 6 replicates (10 ml each), were first stored in test tubes and then analysed on a calibrated hand-held *in vivo* fluorometer (AquaFlor). The fluorescence profiles were normalised with the upstream fluorescence measured in water samples taken every 4 min at the flume entrance. Fluorescence was calibrated with algal concentration measured by means of an electronic particle counter (Elzone).

Filtration activity. Maximal filtration activity of the mussel bed, indicated by maximal valve-opening degrees of the mussels, was stimulated by maintained a supply of algal cells *Rhodomonas* sp. to the flume at concentrations between 2000 and 5000 cells ml^{-1} (equivalent to 2.5 to 6.3 µg Chl *a* l^{-1}; Clausen & Riisgård 1996). Reduced valve-opening degrees of the mussels and thus reduced filtration activity of the mussel bed was induced by algal depletion when stopping the algal supply. Total inactivity of mussels (control scenario) was forced by freezing the mussels on the base plates overnight at −80°C. The valve-opening degrees of the mussels were documented by photoregistering in the central part of the mussel bed every 4 min with a digital camera. The pictures were analysed for the relative distance between valves of individual mussels over time using an imaging program (ImageJ). For each mussel, a fixed point on each of the valves was chosen and the distance between them measured over time to get the relative distance.

The necessity to maintain a certain concentration of silt in the water during ADV measurements stimulated the production of pseudofaeces by the mussels, but this appeared not to affect the mussels since it only caused transient (5 to 15 min) reductions in the valve opening degree on a few occasions.

Analysis of flow data. The mean wall shear stress (τ_w) for the mussel bed was estimated from the momentum-integral equation for incompressible boundary layer flow (Schlichting 1968, p. 146):

$$\tau_w = \rho\frac{\mathrm{d}(U^2\theta)}{\mathrm{d}x} + \rho\delta^* U\frac{\mathrm{d}U}{\mathrm{d}x}; \qquad \delta^* = \int_0^\infty\left(1-\frac{\bar{u}}{U}\right)\mathrm{d}z;$$

$$\theta = \int_0^\infty\frac{\bar{u}}{\bar{U}}\left(1-\frac{\bar{u}}{U}\right)\mathrm{d}z \tag{1}$$

where δ^* is the boundary layer displacement thickness and θ the momentum thickness, both calculated from finite difference approximations of measured $\bar{u}(z)$ profiles and with knowledge of the free stream velocity (U) at the edge of the benthic boundary layer. Note that of the 2 contributions to τ_w in Eq. (1), the first term accounts for the momentum change whereas the second term accounts for any favourable pressure gradient in the flow. The mean drag coefficient for the mussel bed of length L was expressed as:

$$C_D = \frac{1}{\frac{1}{2}\rho U^2 L}\int_0^L \tau_w \mathrm{d}x \tag{2}$$

According to Green et al. (1998), the drag coefficient is a measure of 'the proportion of mean-flow kinetic energy dissipated in the benthic boundary layer by turbulence'. Local turbulent mixing in the flow was estimated by the eddy viscosity (ν_T) according to the Boussinesq approximation (Munson et al. 2002):

$$\nu_T = \frac{-\overline{u'w'}}{\partial\bar{u}/\partial z} \tag{3}$$

where $\overline{u'w'}$ is the covariance between axial and vertical velocity components. In turbulent flow, the instantaneous velocity (u) is decomposed into mean velocity ($\bar{u}$) and fluctuating velocity (u'): $u = \bar{u} + u'$. The turbulence intensity therefore is positively correlated to the variance ($\overline{u'^2}$). It can be evaluated for all 3 velocity components u, v and w in the axial (x), transverse (y) and vertical (z) directions; hence the turbulent kinetic energy can be calculated as:

$$\mathrm{TKE} = \frac{1}{2}(\overline{u'^2} + \overline{v'^2} + \overline{w'^2}) \tag{4}$$

In benthic boundary layer flows dominated by viscous effects, $-\overline{u'w'}$ is expected to be positive, since the local vertical gradient in mean velocity is positive, $\partial\bar{u}/\partial u > 0$, and a downward directed fluctuation ($w' < 0$) will bring fluid of a higher velocity to a region of lower velocity ($u' > 0$) and vice versa. A simple measure for the down-mixing-time, i.e. the time it takes for an algal cell to diffuse from the boundary layer edge at height δ to the mussel bed at height z_1, is expressed by averaging the formula of Ackerman et al. (2001, Eq. [7] therein):

$$t_{mix} = (\delta - z_1)^3 \Big/ \int_{z_1}^{\delta}\nu_T\,\mathrm{d}z \tag{5}$$

Analysis of concentration data. The local value of area-specific algal depletion rate is denoted by $F(x)$ ($m^3\ m^{-2}\ s^{-1}$). Since *Rhodomonas* sp. is completely retained by *Mytilus edulis* (Møhlenberg & Riisgård 1978), the concentration integral equation for the boundary layer becomes:

$$\frac{\mathrm{d}}{\mathrm{d}x}\left(\int_0^\infty [C_\infty - C(x,z)]\bar{u}(x,z)\,\mathrm{d}z\right) = C_w(x)F(x) \tag{6}$$

where C_∞ denotes the mean algal concentration in the free stream, $C_w(x)$ that at the mussel bed, and $\bar{u}$ the local mean velocity in x. Note that F should equal the estimated area-specific population-filtration rate (F_{pop}) for 100% particle retention efficiency and a uniform concentration C_∞. But because of the development of a concentration boundary layer, $C_w(x)$ will be less than C_∞ and it will decrease for increasing x. For this reason,

$F(x)$ may not equal the full potential F_{pop}. Dividing Eqn (6) by C_∞ and integrating from $x = 0$ to $x = L$ gives:

$$\int_0^\infty [1 - C(L,z)/C_\infty]\,\bar{u}(L,z)\,dz = \int_0^L [C_w(x)/C_\infty]\,F(x)\,dx \equiv LF_m(L) \quad (7)$$

where $F_m(L)$ defines the average value of the area-specific algal depletion rate over the length L. The left part of Eq. (7) may be obtained from experimental data for different scenarios. The ratio $F_m(L)/F_{pop}$ is the fraction of the potential feeding rate that is actually achieved across the length L of the mussel bed. F_m will decrease with increasing L, whereas the quantity LF_m that represents the total depletion will increase.

Uncertainty estimates. The autocorrelation function for velocity data revealed a typical integral time scale of $T_0 = 0.6$ s. With a Nyquist frequency of $1/2T_0 = 1/(2 \times 0.6\ s) = 0.8$ Hz and a sampling interval of 30 s the effective sample size becomes $N_{eff} = 0.8\ Hz \times 30\ s = 24$. Relative uncertainties (S,%) for recorded time-series of mean velocity ($\bar{u}$), velocity variance ($\overline{u'u'}$) and velocity covariance ($\overline{u'w'}$) were estimated according to Benedict & Gould (1996) (Table 2). The standard deviations in concentration data, calculated from 6 replicates, were less than 8%.

Table 2. *Mytilus edulis*. Relative uncertainties of flow data (see text for explanations)

Flow	$S(\bar{u})$ (%)	$S(\overline{u'u'})$ (%)	$S(-\overline{u'w'})$ (%)
Fast	5	29	34
Slow	5	29	14

RESULTS

Fig. 2 shows the change in upstream algal concentrations and mean valve-opening degree of the video-recorded mussels in the slow and fast flow flume experiments. The addition of algal culture resulted in maximal valve-opening degrees and hence maximal filtration activity after about 1 h, which lasted as long as the algal supply to the flume was maintained. More generally, the point of maximal filtration activity of the mussel bed is seen as the algal concentration enters a steady state at t = 170 min for the slow flow and t = 110 min for the fast flow flume experiment. At the end of the experiments, the valve gapes gradually decreased as the algal concentration was depleted by the mussels.

The general flow characteristics of the developing boundary layer over the mussel bed are shown in Fig. 3 in terms of contours of normalized mean axial velocity ($\bar{u}/U$). The contours in Fig. 3 suggest increasing boundary layer thickness both with downstream position and with level of mussel activity. These trends are quantified in Fig. 4 in terms of the momentum thickness (θ) given in Eq. (1), which shows little difference between slow and fast flow but a clear increase with increasing activity of mussels. The observed increment in θ (increasing momentum deficit in the boundary layer) with increasing mussel activity signals increasing wall drag, as shown in Fig. 5a. Here, the mean wall shear stress τ_w/ρ (the square of friction velocity, u^{*2}) averaged over the length of the mussel bed was calculated from Eq. (1) to demonstrate the effect of biomixing. For both slow and fast flow, τ_w/ρ more than doubles as filtration activity increases from zero to the maximal level. Table 3 gives contributions to τ_w/ρ from first and second term in Eq. (1), as well as the mean drag coefficient (C_D) from Eq. (2).

Because of the relatively high uncertainty of the present data for velocity covariance ($\overline{u'w'}$) only the average level of the eddy viscosity (ν_T) Eq. (3) as appearing in the expression Eq. (5) for the down-

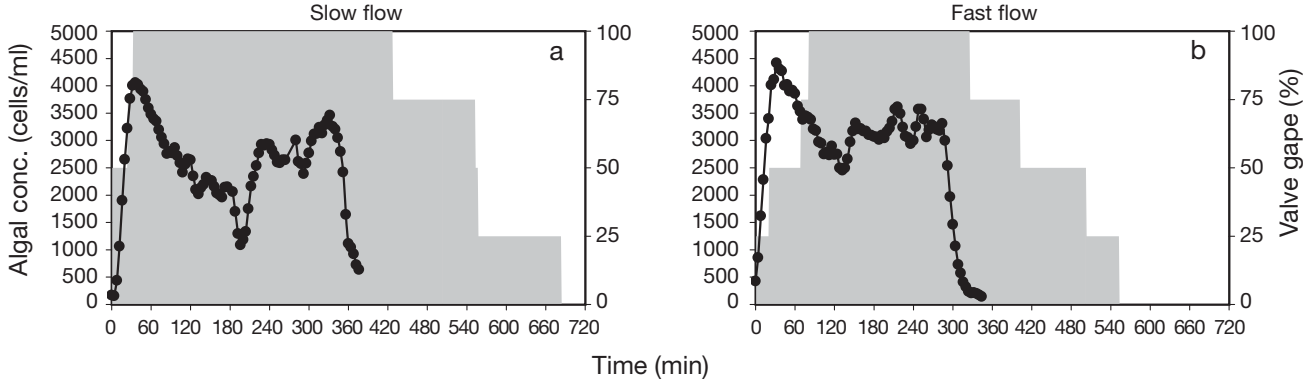

Fig. 2. *Mytilus edulis*. Filtration activity after addition of algal cells *Rhodomonas* sp. at time 0 (T_0) in 2 flume experiments conducted at (a) slow (4 cm s^{-1}) and (b) fast (8 cm s^{-1}) flow speeds. Curves show the upstream algal concentration. Algal dosing was stopped at time 336 min at slow flow and 284 min at fast flow. Background bars show the mean valve-opening degree of mussels (slow flow: n = 4 ind., fast flow: n = 5 ind.) on an interval scale

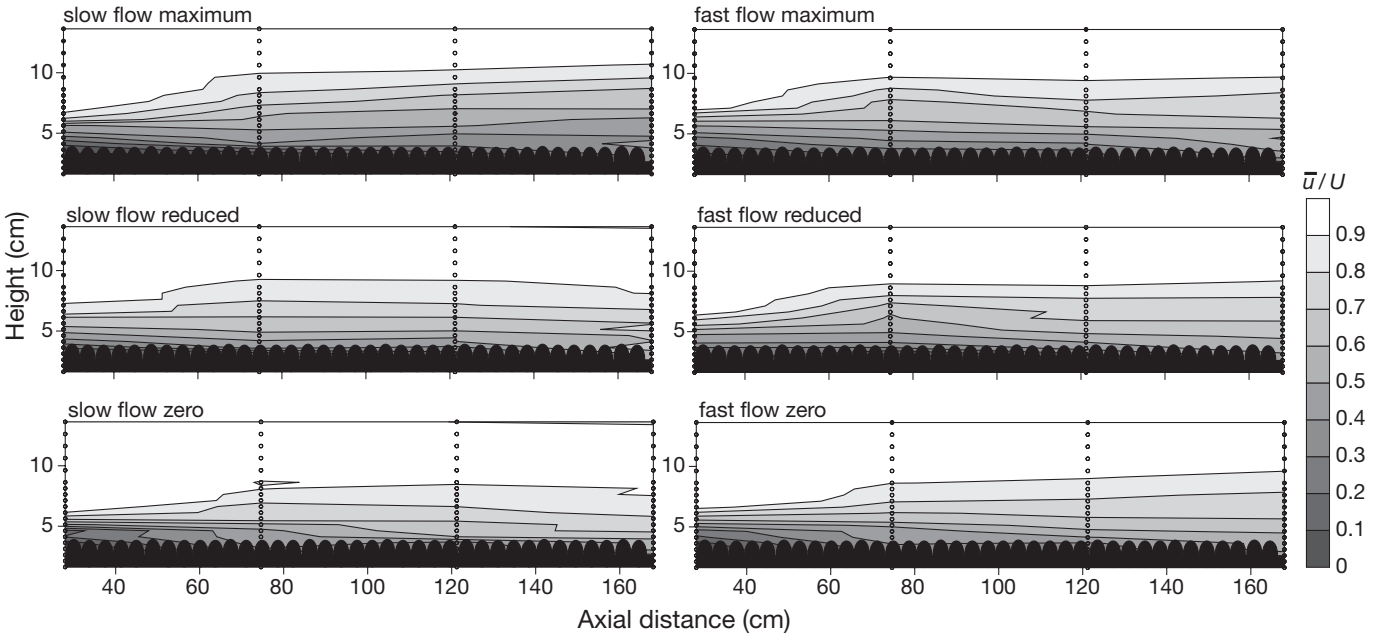

Fig. 3. Contours of normalized mean axial velocity ($\bar{u}/U$) for the 3 × 2 experimental matrix: fast and slow flow speeds, and maximal, reduced and zero filtration activity. Leading edge of mussel bed: $x = 0$. Flume floor: $z = 0$. Average height of mussel bed $z = 3.9 \pm 1.1$ cm

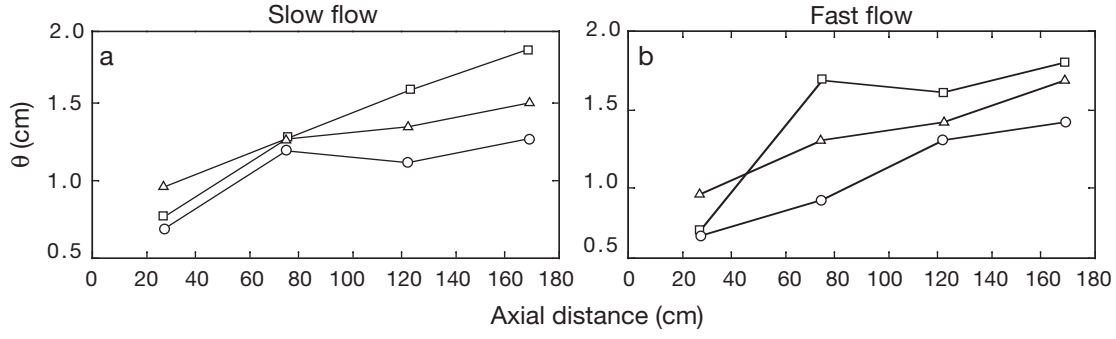

Fig. 4. Momentum thickness (θ) from Eq. (1) for maximal (□), reduced (△) and zero (○) filtration activity of mussels versus length of mussel bed. (a) Slow; (b) fast flow

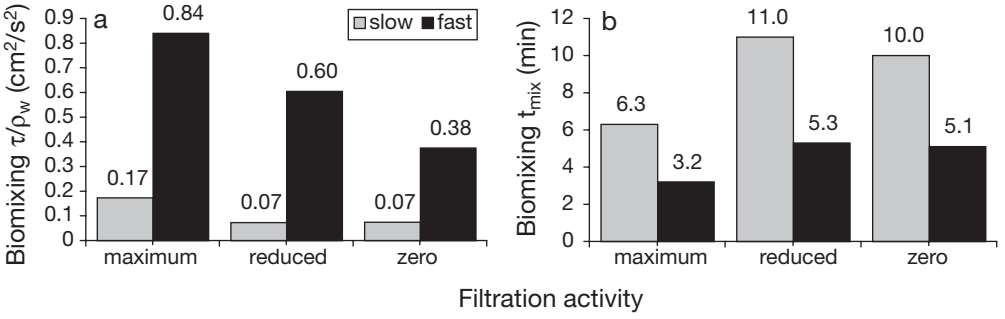

Fig. 5. Biomixing indicators versus filtration activity for slow and fast flow. (a) $\tau_w/\rho = u_*^2$ from Eq. (1) (average over length). (b) t_{mix} from Eq. (5) at $x = 168$ cm

mixing-time (t_{mix}) has been evaluated, using the height interval from 3.63 to 13.63 cm above the flume floor in the integral in Eq. (5). As shown in Fig. 5b t_{mix} tends to decrease with increasing filtration activity and more so for slow flow than for fast flow. The values at slow flow are about twice those of fast flow, indicating the inverse of the approximate levels of ν_T for the 2 flows.

Further detailed characteristics of the benthic boundary layer at the downstream position (x = 162 to 168 cm) are shown in Fig. 6. It shows vertical profiles of the flow-related parameters: normalised axial velocity ($\bar{u}/U$), Reynolds stress ($-\overline{u'w'}$), turbulent kinetic energy (TKE), and normalized algal concentration (C/C_0). Gliding averages are shown in the figure to filter scatter in the raw data and thus to indicate the general trends. Profiles shown with dashed lines represent reference data for flume flow over a bare sand floor. The effect of maximal filtration activity is most pronounced for slow flow where, in a wide region ($z \approx 5$ to 10 cm), $\bar{u}/U$ is reduced while $-\overline{u'w'}$ and TKE are significantly increased. The latter trend is also present for the fast flow, but occurs closer to the bed. The concentration profiles for maximal filtration activity show lower values near the mussel bed for slow flow than for fast flow (C_w/C_0 in Eq. 7), i.e. a higher degree of refiltration.

The general concentration characteristics of the boundary layer are shown in Fig. 7 in terms of contours of C/C_0 above the mussel bed for maximal filtration activity at slow and fast slow. For slow flow, the algal-concentration boundary layer is thicker and the concentration gradients towards the mussel bed are

Table 3. *Mytilus edulis*. Ratio of wall shear stress (τ_w) from Eq. (1) and density of water (ρ), and drag coefficient (C_D) from Eq. (2) for the 3 × 2 experimental matrix. τ_w/ρ and C_D are averaged over the length of mussel bed. Contributions to τ_w/ρ: from momentum changes (Term 1) and from pressure gradient (Term 2) in Eq. (1)

Filtration activity	τ_w/ρ (cm^2 s^{-2})	Term 1 (cm^2 s^{-2})	Term 2 (cm^2 s^{-2})	C_D –
Slow flow				
Maximal	0.173	0.153	0.020	0.018
Reduced	0.073	0.071	0.002	0.008
Zero	0.074	0.091	−0.017	0.009
Fast flow				
Maximal	0.840	0.751	0.089	0.018
Reduced	0.604	0.436	0.168	0.014
Zero	0.375	0.394	−0.019	0.010

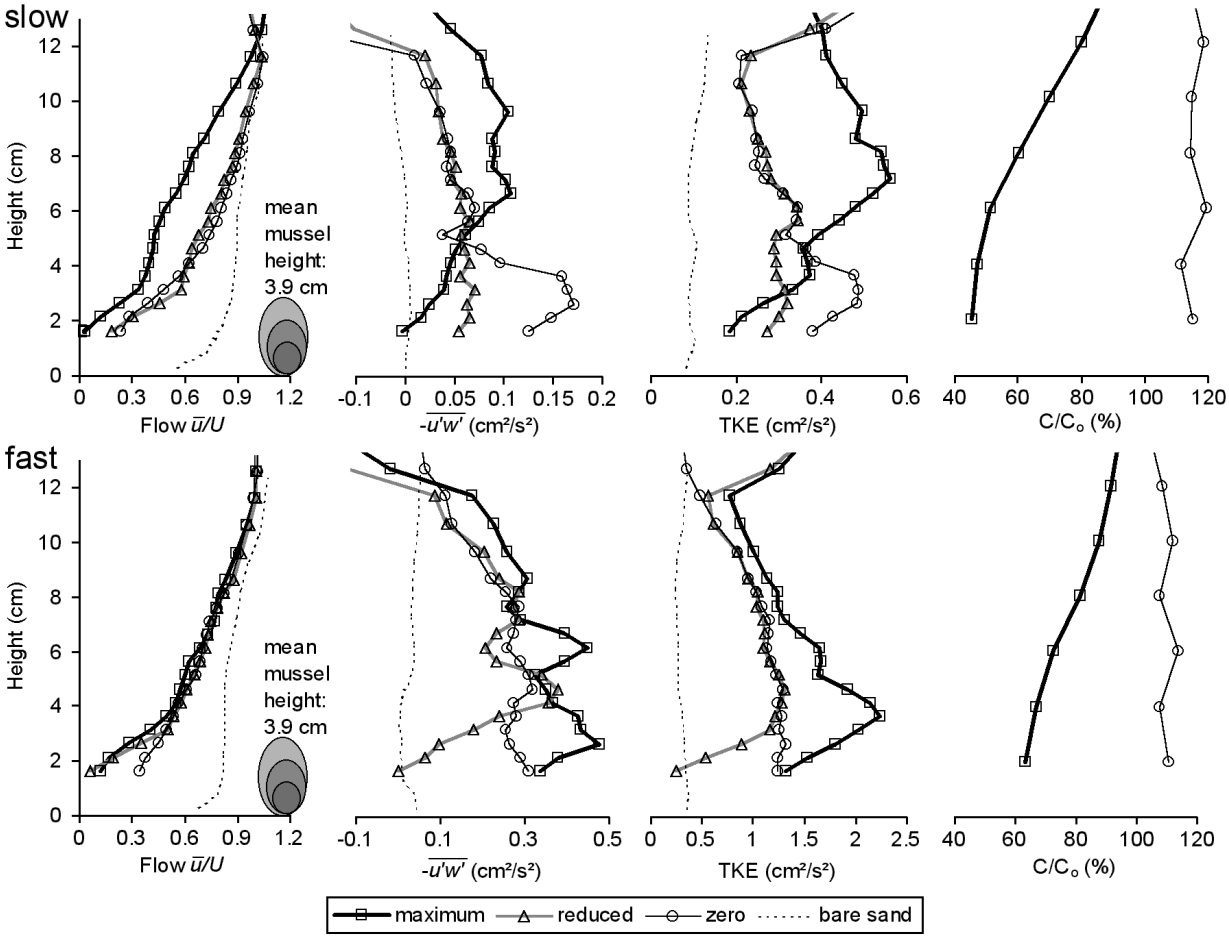

Fig. 6. Vertical profiles downstream (x = 162 to 168 cm) for slow and fast flow. Left to right: normalized mean axial velocity ($\bar{u}/U$), velocity covariance ($-\overline{u'w'}$), turbulent kinetic energy (TKE), and normalized mean concentration (C/C_0) versus height above plume floor. Maximum (□), reduced (△) and zero (○) filtration activity. Dashed lines show profiles for a bare sand flume floor

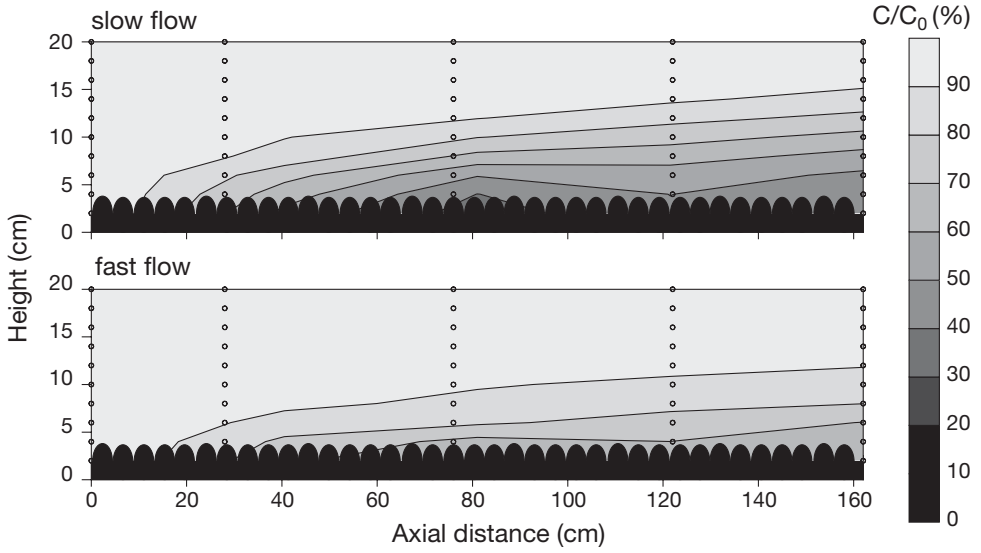

Fig. 7. Contours of normalized mean algal concentration (%, C/C_0) for slow and fast flow at maximal filtration activity

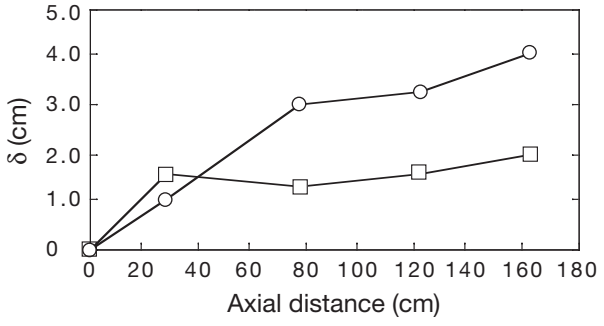

Fig. 8. Concentration-displacement thickness (δ_C) versus length of mussel bed for slow (○) and fast (□) flow speeds at maximal filtration activity

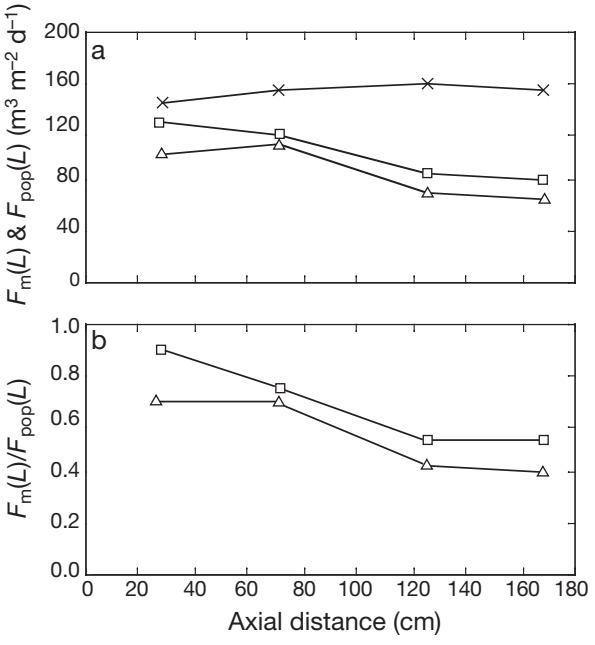

Fig. 9. Grazing impact of mussel bed at maximal filtration activity. (a) Estimated area-specific population-filtration rate (F_{pop}) (×) and area-specific depletion rate (F_m from Eq. 7) at slow (△) and fast (□) flow speed. (b) Ratio $F_m(L)/F_{pop}(L)$ versus length of mussel bed at slow (△) and fast (□) flow

less steep. The development of the concentration boundary layers is quantified in Fig. 8 in terms of the concentration-displacement thickness, defined as $\delta_C = \int(1 - C/C_0)dz$ in analogy to δ^* from Eq. (1), revealing the greater thickness and more rapid growth for the case of slow flow. Fig. 9a shows the computed area-specific population-filtration rate ($F_{pop}(L)$; see Table 1) and the area-specific algal depletion rate (F_m (L)) from Eq. (7) averaged over increasing distances from the leading edge of the mussel bed. Fig. 9b shows that the ratio $F_m(L)/F_{pop}(L)$ at slow and fast flow decreased along the mussel bed from a theoretical value of unity at the leading edge of the bed to 0.42 at slow and 0.55 at fast flow at the downstream position (x = 162 cm), which implies a depletion of about 58 and 45%, respectively.

The effect of biomixing of the mussel bed on the structure and thickness of the algal-concentration-boundary layer was also investigated during the transient phase of stimulation of the mussels to reach the steady state of maximal filtration activity in the slow-flow experiment. At the downstream position (x = 162 cm), Fig. 10 shows how the concentration-boundary layer grows thicker with less steep vertical gradients as the mussels increase their filtration activity. The thickness of the algal concentration-boundary layer approaches the steady state limit at $t \approx 170$ min. At this time the upstream algal concentration enters a steady state and therefore the whole mussel bed has reached maximal filtration activity and hence maximal biomixing effect.

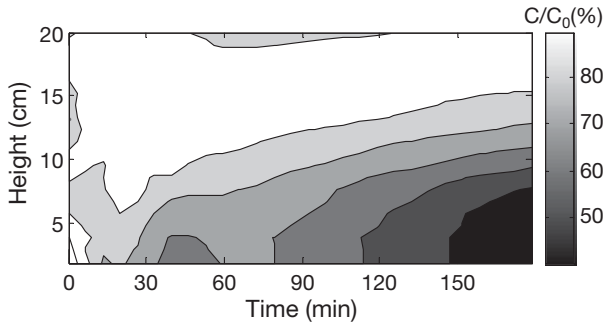

Fig. 10. Transient development of algal concentration-boundary layer downstream (x = 162 cm) during the opening phase of the mussels prior to the slow-flow flume experiment (time period 0 to 180 min of Fig. 2a)

DISCUSSION

In the present flume study natural food and flow conditions were established for the mussels. By keeping the algal concentration within a natural (low) range of 1.0 to 6 µg Chl *a* l^{-1} the mussels were stimulated to open wide and pump at a maximal rate, whereas starvation conditions at depleted algal concentrations resulted in reduced valve gapes (Fig. 2). The observed pattern of mussel-filtration activity in relation to algal concentration agrees with the experimental work of Riisgård et al. (2003) and confirms that mussels are adapted to continuous filter feeding at naturally low algal concentrations (Jørgensen et al. 1986, Riisgård & Larsen 1995, 2001, Riisgård 2001a,b).

The experimental results of the present flume study fall into 2 parts: the momentum transport (which is purely fluid mechanical and involves distributions of quantities such as velocity, turbulence intensity and shear stress), and the mass transport (which involves distributions of algal concentration and fluxes). For 2 flow speeds (slow and fast), the momentum transport was studied at 3 levels of mussel activity (maximal, reduced and zero) to reveal systematic trends with decreasing filtration activity. However, the mass transfer was only studied for the maximal and zero mussel activity. The 2 parts are related by the Reynolds analogy, hypothesising proportionality between momentum and mass transport, particularly for the eddy diffusivity of momentum to be proportional to the eddy diffusivity of mass. These considerations are implicit in the following discussion.

Biomixing caused by exhalant jets and inhalant suction from individual mussels in a dense population can increase the down-mixing of phytoplankton to the bed in turbulent channel flow conditions. This is concluded from observed increases in turbulent kinetic energy (TKE) and Reynolds stress ($-\overline{u'w'}$) (Fig. 6), which implies increased mixing that leads to an increased momentum thickness (θ) of the benthic boundary layer (Fig. 4). An additional indication of increased mixing and dissipation due to exhalant jets of mussels is increased wall shear stress and drag (Fig. 5a; Table 3). Note that the contribution to wall shear stress (τ_w) from a pressure gradient (second term in Eq. (1), see Table 3) is not negligible at fast flow and maximal mussel activity, which may reflect the relatively shallow flume flow. The average value of the friction velocity ($u^* = (\tau_w/\rho)^{1/2}$) over the length of the mussel bed increased by 56% (from 0.26 to 0.41 cm s^{-1}) for slow flow and 49% (from 0.62 to 0.92 cm s^{-1}) for fast flow during change from zero to maximal mussel filtration activity. For a comparison to natural flow conditions, field velocity profiles have revealed magnitudes of u^* in the range of 0.25 to 2 cm s^{-1} above beds of blue mussels *Mytilus edulis*, horse mussels *Atrina zelandica* and populations of cockles *Cerastoderma edule* in tidal regimes (Fréchette et al. 1989, Newell & Shumway 1993, Green et al. 1998, Jonsson et al. 2001, Nikora et al. 2002). The matching of present magnitudes of u^* with field values suggests that natural near-bottom flow conditions were reproduced in the present flume study.

Added mixing in turbulent flow caused by biomixing was about the same at slow and fast flow, as can be seen from the computed down-mixing time (t_{mix}) based on the eddy diffusivity of momentum (ν_T) calculated from the data (Fig. 5b). In fact, t_{mix} is merely the reciprocal of a suitable average of ν_T. The decrease in t_{mix} in scenarios from zero to maximal filtration activity amounted to a factor of about 1.6 for both flows, but biomixing reached further into the flow for slow than for fast flow. This shows the functionality of biomixing to be more helpful for the mussels at low speed where it is most needed due to a lower level of flow-induced turbulence that contributes to down-mixing of phytoplankton.

The Reynolds stress and TKE peak in the region between 5 and 10 cm and between 3 and 6 cm above the mussel bed at slow and fast flow, respectively (Fig. 6), are interpreted as approximate 'penetration heights' of the exhalant jets. This is analogous to the peak in Reynolds stress observed above benthic aquatic vegetation (Nepf & Vivoni 2000) and indicates that a turbulent shear layer is generated near the top of penetration of exhalant jets into the flow. The higher penetration height at slow flow was expected due to a larger ratio of velocity of exhalent jet to axial velocity. According to O'Riordan et al. (1993, 1995) the height where maximal algal depletion occurs above benthic filter feeders is generally confined to the inner boundary layer below a dimensionless height $z+$ of 600, where $z+ = u^*z/\nu$, (u^* = friction velocity, z = height above bottom, and ν = kinematic viscosity of water). In particular, O'Riordan et al. (1993) found a dimension-

less jet penetration height of magnitude around 300 for model clams with exhalant jet velocities of 9.8 cm s^{-1} under flume-flow conditions with $u^* = 0.4$ cm s^{-1}. For the present case of slow flow with $u^* = 0.41$ cm s^{-1} the dimensionless jet-penetration height is of the same order of magnitude (294 to 336) as found by these authors, whereas for fast flow with $u^* = 0.92$ cm s^{-1} the magnitude of the dimensionless jet-penetration height is larger (364 to 455). However, because of the hydrodynamic differences between model siphons protruding from a smooth bottom and live mussels forming a rough bottom a direct comparison of results may be fortuitous.

In calculating the down-mixing time the present eddy-viscosity (ν_T) values were found to be of the order of 0.4 and 0.6 cm^2 s^{-1} for slow and fast flow, respectively. These values may be compared to 1.50 cm^2 s^{-1} found for stagnant water above a population of ascidians *Ciona intestinalis* filtering at $F_{pop} = 6.72$ m^3 m^{-2} d^{-1} (Larsen & Riisgård 1997), which is an order of magnitude to be predictable by simple scaling: $\nu_T \approx 0.1 \times d_{jet} \times u_{jet}$, where d_{jet} and u_{jet} denote the diameter and velocity, respectively, of the exhalant jet. Applying this scaling to the exhalant jet of *Mytilus edulis*, gives the estimate $\nu_T = 0.1 \times 0.4 \times 8 = 0.32$ cm^2 s^{-1}, which is about 80% of the value obtained for slow flow, and about 53% of that for fast flow. These fractions may be interpreted as being the relative importance of biomixing, which therefore plays a greater role for slow flow. However, the contributions to mixing from the 2 mechanisms interact and cannot be simply superposed. Only a detailed numerical calculation of the turbulent boundary layer over a rough surface, with and without an account of an array of inhalant and exhalant feeding currents, could possibly resolve the question of the interaction of the 2 mixing mechanisms.

Numerical 2-dimensional modelling of zoobenthic grazing impacts has until now assumed a logarithmic velocity profile and a linearly decreasing turbulent shear stress from the bottom to the surface (Fréchette et al. 1989, Dade 1993, Butman et al. 1994). The present study shows that the effect of biomixing changes the vertical Reynolds-stress profile from a nearly linear towards a parabolic distribution that peaks highest above the bottom for slow flow (Fig. 6). The same trend is seen in the detailed Reynolds stress data in van Duren et al. (2005) for flume flow over a bed of filter-feeding *Mytilus edulis*, where peaks in Reynolds stress due to filtering activity are still closer to the bottom because of the higher flow speeds ($u^* \approx 4$ to 40 cm s^{-1}). Their velocity data showed a double log-layer at low or no activity, but a single log-layer for actively filtering mussels. Therefore, the existing 2-dimensional modelling may be used as a first approach to evaluate the effect of biomixing on grazing impacts of mussel beds. In a model setup for a mussel bed with water depth 2.25 m and surface velocity 30 cm s^{-1}, Fréchette et al. (1989, their Fig. 9) simulated a 15% increase in local mussel bed consumption rate at 50 m downstream the mussel bed when increasing u^* by 50% (i.e. from 0.98 to 1.55 cm s^{-1}) through an increase in the hydraulic roughness. Since biomixing may increase u^* with 50%, as found in the present study, this is a strong indication that biomixing plays an essential role in the nutrition of dense mussel populations, and therefore biomixing has to be taken into account when estimating, for example, the carrying capacity of coastal areas for mussel beds and aquaculture sites with line-cultures of mussels, because carrying capacity is limited not only by large scale processes governed by water exchange and primary production but also by small-scale processes such as insufficient mixing of water (Smaal et al. 1998, Pilditch et al. 2001). In a recent work by Tweddle et al. (2005) time series of tidal-current generated Reynolds stress measured by acoustic Doppler in the field showed a positive correlation with vertical mixing of the phytoplankton biomass. Thus food depletion above a mussel bed was found to coincide with events of negligible levels of Reynolds stress.

The measured distributions of algal concentration show that the algal concentration-boundary layer is thicker at slow flow than at fast flow (Figs. 6 to 8) and that the algal concentration near the mussel bed (C_w/C_∞ in Eq. 7) is lower for slow flow than for fast flow. This implies a higher degree of refiltration at slow flow, as also found by O'Riordan et al. (1993, 1995) in their flume studies of concentration-boundary layer dynamics over models of endo-benthic filter-feeding bivalves. In fact, the refiltration fraction (C_w/C_∞) should increase with increasing velocity ratio, VR = u_{jet}/u^* (jet to friction velocity) for VR < 20 for extended siphons according to these authors, which is in agreement with the present results for slow and fast flow, showing the approximate values VR = 8/0.41 = 19 and 8/0.92 = 8.7, respectively, based on bed-averaged u^* values. Also, the area-specific algal depletion rate (F_m) calculated from the data (Fig. 9) correlates positively with velocity and mixing in the benthic boundary layer, F_m/F_{pop} reaching the value of 0.42 and 0.55 at slow and fast flow, respectively, at the downstream position (x = 162 cm). The average food uptake of the mussel bed at slow flow is thus about 80% of that at fast flow, even though C_w at slow flow is only about 67% of that at fast flow. So, the higher degree of refiltration at slow flow is partially being compensated for by an effective biomixing, which reaches far into the flow causing increased down-mixing of phytoplankton.

From a biological point of view the upstream mussels in a bed experience little refiltration, hence are ensured a high feeding rate. Mussels further down-

stream, however, experience increasing refiltration, hence decreasing feeding rates, due to the development of a concentration-boundary layer (i.e. along with the horizontal and vertical reduction in algal concentration). The present study shows that refiltration due to insufficient mixing tends to level off for beds longer than about 150 cm (Fig. 9). The reason for this is partly the turbulent mixing due to wall roughness represented by the mussels (e.g. Asmus & Asmus 1991, Crimaldi et al. 2002), and partly the biomixing effect. However, to evaluate the importance of biomixing in the field, particularly on a large scale, the influence of a number of additional factors should be known. These factors include: topology and size of mussel bed, food quality and quantity including effect of suspended matter, and changing direction and strength of flow including oscillations. For the time being, at least for steady flow conditions, it appears that the pragmatic model of Fréchette et al. (1989) may provide reasonable estimates of food uptake and depletion, provided that the required augmentation of u^* due to biomixing can be properly estimated. The present flume study contributes with explicitly measured values of this augmentation, although only for 2 flows, and more data are required, including the verification of a possible downstream asymptotic 'state of no further development' of the boundary layer and depletion.

Acknowledgements. The EU network BioFlow (contract no. EVR1-CT-2001-20008) provided a part of the funding for this study. H.U.R. was funded by a grant from the Danish Natural Science Research Council (grant no. 51-00-0314). We acknowledge Holger Pielenz for his help with the technical aspects and for providing his camera. Furthermore, we thank the 4 reviewers for their pertinent and useful comments and suggestions.

LITERATURE CITED

Ackerman JD, Loewen MR, Hamlin PF (2001) Benthic-pelagic coupling over a zebra mussel reef in western Lake Erie. Limnol Oceanogr 46:892–904

Asmus RM, Asmus H (1991) Mussel beds: limiting or promoting phytoplankton? J Exp Mar Biol Ecol 148:215–232

Benedict LH, Gould RD (1996) Towards better uncertainty estimates for turbulence statistics. Exp Fluids 22:129–136

Butman CA, Fréchette M, Geyer WR, Starczak VR (1994) Flume experiments on food supply to the blue mussel *Mytilus edulis* L. as a function of boundary–layer flow. Limnol Oceanogr 39:1755–1768

Clausen I, Riisgård HU (1996) Growth, filtration and respiration in the mussel *Mytilus edulis*: no evidence for physiological regulation of the filter-pump to nutritional needs. Mar Ecol Prog Ser 141:37–45

Crimaldi JP, Thompson JK, Rosman JH, Lowe RJ, Koseff JR (2002) Hydrodynamics of larval settlement: the influence of turbulent stress events at potential recruitment sites. Limnol Oceanogr 47:1137–1151

Dade WB (1993) Near-bed turbulence and hydrodynamic control of diffusional mass transfer at the sea floor. Limnol Oceanogr 38:52–69

Dolmer P (2000) Algal concentration profiles above mussel beds. J Sea Res 43:113–119

Forster S, Zettler ML (2004) The capacity of the filter-feeding bivalve *Mya arenaria* L. to affect water transport in sandy beds. Mar Biol 144:1183–1189

Fréchette M, Butman CA, Geyer WG (1989) The importance of boundary-layer flows in supplying phytoplankton to the benthic suspension feeder, *Mytilus edulis* L. Limnol Oceanogr 34:19–36

Fréchette M, Bourget E (1985) Energy flow between the pelagic and benthic zones: factors controlling particulate organic matter available to an intertidal mussel bed. Can J Fish Aquat Sci 42:1158–1165

Friedrichs M, Graf G (2006) Description of a flume channel profilometry tool using laser line scans. Aquat Ecol, BioFlow Spec Iss (in press)

Green MO, Hewitt JE, Thrush SF (1998) Seabed drag coefficient over natural beds of horse mussels (*Atrina zelandica*). J Mar Res 56:613–637

Herman PMJ, Middelburg JJ, Koppel JV, Heip CHR (1999) Ecology of estuarine macrobenthos. Adv Ecol Res (29): 195–240

Jonsson PR, Petersen JK, Karlsson Ö, Loo LO, Nielsson S (2005) Particle depletion above experimental bivalve beds: in situ measurements and numerical modeling of bivalve filtration in the boundary layer. Limnol Oceanogr 50:1989–1998

Jørgensen CB (1984) Effect of grazing: metazoan suspension feeders. In: Hobbie JE, Williams PJ (eds) Heterotrophic activity in the sea. Plenum Press, New York, p 445–464

Jørgensen CB (1990) Bivalve filter feeding: hydrodynamics, bioenergetics, physiology and ecology. Olsen & Olsen, Fredensborg

Jørgensen CB, Famme P, Kristensen HS, Larsen PS, Møhlenberg F, Riisgård HU (1986) The bivalve pump. Mar Ecol Prog Ser 34:69–77

Larsen PS, Riisgård HU (1997) Biomixing generated by benthic filter-feeders: a diffusion model for near-bottom phytoplankton depletion. J Sea Res 37:81–90

Loo LO, Rosenberg R (1989) Bivalve suspension-feeding dynamics and benthic-pelagic coupling in an eutrophicated marine bay. J Exp Mar Biol Ecol 130:253–276

Mann KH, Lazier JRN (1996) Dynamics of marine ecosystems. Biological–physical interactions in the ocean. Blackwell Scientific Publications, Cambridge, MA, p 1–394

Møhlenberg F (1995) Regulating mechanisms of phytoplankton growth and biomass in a shallow estuary. Ophelia 42: 239–256

Møhlenberg F, Riisgård HU (1978) Efficiency of particle retention in 13 species of suspension feeding bivalves. Ophelia 17:239–246

Monismith SG, Koseff JR, Thompson J, O'Riordan CA, Nepf H (1990) A study of model bivalve siphonal currents. Limnol Oceangr 35:680–696

Munson BR, Young DF, Okiishi TH (2002) Fundamentals of fluid mechanics. John Wiley, River Street, NJ

Nepf HM, Vivoni ER (2000) Flow structure in depth-limited, vegetated flow. J Geophys Res 105:547–557

Newell CR, Shumway SE (1993) Grazing of natural particulates by bivalve molluscs: a spatial and temporal perspective. In: Dame RF (ed) Bivalve filter feeders in estuarine and coastal ecosystem processes. Springer-Verlag, Berlin, p 85–148

Nikora V, Green MO, Thrush SF, Hume TM, Goring D (2002) Structure of the internal boundary layer over a patch of

pinnid bivalves (*Atrina zelandica*) in an estuary. J Mar Res 60:121–150
Norén F, Haamer J, Lindahl O (1999) Changes in the plankton community passing a *Mytilus edulis* mussel bed. Mar Ecol Prog Ser 191:187–194
O'Riordan CA, Monismith SG, Koseff JR (1993) A study of concentration boundary-layer formation over a bed of model bivalves. Limnol Oceangr 38:1712–1729
O'Riordan CA, Monismith SG, Koseff JR (1995) The effect of bivalve excurrent jet dynamics on mass transfer in a benthic boundary layer. Limnol Oceangr 40:330–344
Petersen JK, Riisgård HU (1992) Filtration capacity of the ascidian *Ciona intestinalis* and its grazing impact in a shallow fjord. Mar Ecol Prog Ser 88:9–17
Peterson CH, Black R (1988) Responses of growth to elevation fail to explain vertical zonation of suspension-feeding bivalves on a tidal flat. Oecologia 76:423–429
Pilditch CA, Grant J, Bryan KR (2001) Seston supply to sea scallops (*Placopecten magellanicus*) in suspended culture. Can J Fish Aquat Sci 58:241–253
Riisgård HU (1991) Suspension feeding in the polychaete *Nereis diversicolor*. Mar Ecol Prog Ser 70:29–37
Riisgård HU (1998) Filter feeding and plankton dynamics in a Danish fjord: a review of the importance of flow, mixing and density-driven circulation. J Environ Manage 53: 195–207
Riisgård HU (2001a) On measurement of filtration rates in bivalves — the stony road to reliable data: review and interpretation. Mar Ecol Prog Ser 211:275–291
Riisgård HU (2001b) The stony road to reliable filtration rate measurements in bivalves: a reply. Mar Ecol Prog Ser 211: 275–291
Riisgård HU, Larsen PS (1995) Filter-feeding in marine macro-invertebrates: pump characteristics, modelling and energy cost. Biol Rev 70:67–106
Riisgård HU, Larsen PS (2001) Minireview: Ciliary filter feeding and bio-fluid mechanics — present understanding and unsolved problems. Limnol Oceanogr 46:882–891
Riisgård HU, Randløv A (1981) Energy budgets, growth and filtration rates in *Mytilus edulis* at different algal concentrations. Mar Biol 61:227–234
Riisgård HU, Seerup DF (2003) Filtration rates in soft clam, *Mya arenaria*: effects of temperature and body size. Sarsia 88:425–428
Riisgård HU, Jürgensen C, Clausen T (1996a) Filter-feeding ascidians (*Ciona intestinalis*) in a shallow cove: implications of hydrodynamics for grazing impact. J Sea Res 34: 293–300
Riisgård HU, Poulsen L, Larsen PS (1996b) Phytoplankton reduction in near-bottom water caused by filter-feeding *Nereis diversicolor*—implications for worm growth and population grazing impact. J Sea Res 35:293–300
Riisgård HU, Jensen AS, Jürgensen C (1998) Hydrography, near-bottom currents, and grazing impact of the filter-feeding ascidian *Ciona intestinalis* in a Danish fjord. Ophelia 49:1–16
Riisgård HU, Kittner C, Seerup DF (2003) Regulation of the opening state and filtration rate in filter-feeding bivalves (*Cardium edule*, *Mytilus edulis*, *Mya arenaria*) in response to low algal concentration. J Exp Mar Biol Ecol 284: 105–127
Riisgård HU, Seerup DF, Jensen MH, Glob E, Larsen PS (2004) Grazing impact of filter-feeding zoobenthos in a Danish fjord. J Exp Mar Biol Ecol 307:261–171
Schlichting H (1968) Boundary layer theory. McGraw-Hill, New York
Smaal AC, Prins TC, Dankers N, Ball B (1998) Minimum requirements for modelling bivalve carrying capacity. Aquat Ecol 31:423–428
Springer B, Friedrichs M, Graf G, Nittikowski J, Queisser W (1999) A high-precision current measurement system for laboratory flume systems: A case study around a circular cylinder. Mar Ecol Prog Ser 183:305–310
Tweddle JF, Simpson JH, Janzen CD (2005) Physical controls of food supply to benthic filter feeders in the Menai Strait, UK. Mar Ecol Prog Ser 289:79–88
van Duren LA, Herman PMJ, Sandee AJJ, Heip CHR (2006) Effects of mussel filtering activity on boundary layer structure, J Sea Res 55:3–14
Vogel S (1994) Life in moving fluids. The physical biology of flow. Princeton University Press, Princeton, NJ
Wildish D, Kristmanson D (1984) Importance to mussel of the benthic boundary layer. Can J Fish Aquat Sci 41: 1618–1625
Wildish D, Kristmanson D (1997) Benthic suspension feeders and flow. Cambridge University Press, Cambridge

Editorial responsibility: Howard I. Browman (Associate Editor-in-Chief), Storebø, Norway

Submitted: May 3, 2005; Accepted: November 3, 2005
Proofs received from author(s): April 18, 2006